ChemCatChem

Research Article
doi.org/10.1002/cctc.202401405

Chemistry Europe
European Chemical Societies Publishing

www.chemcatchem.org

Process Understanding of Transamination Reaction in Chiral Pharmaceutical Intermediate Production Catalyzed by an Engineered Amine Transaminase

Zeynep Perçin,*[a] Florian Kleinbeck,[b] Paul Bubenheim,[a] Thomas Ruch,[b] and Andreas Liese*[a]

Chiral amines are key building blocks for the synthesis of many active pharmaceutical ingredients (APIs). Biocatalytic routes offer significant advantages to provide sustainable access to such motifs on commercial scale, with sacubitril valsartan sodium hydrate as a recent example. In this study a deeper mechanistic and kinetic understanding of the central biocatalytic step in the synthesis of sacubitril valsartan sodium hydrate, applying the evolved transaminase CDX-043, was gained. The equilibrium of the transamination reaction was investigated in detail, and two kinetic models (ping-pong two-substrate kinetics and Michaelis–Menten double substrate kinetics) were established, considering substrate and product inhibition. The determined equilibrium constant indicates that the equilibrium lies strongly on the product side. The results of the kinetic studies demonstrate that the transaminase reaction is in conformity with the Michaelis–Menten double substrate kinetic model. Product inhibition was found to be more severe than substrate inhibition. The application of a plug flow reactor (PFR) was shown to be the preferred reactor setup to reduce the occurring inhibition.

1. Introduction

Chiral amines are ubiquitously found as structural motifs in active pharmaceutical ingredients (APIs), with access routes often relying on primary amines as key intermediates. To meet the constantly increasing requirements for efficiency and sustainability, biocatalytic approaches—and among them in particular transaminases—have emerged for commercial manufacture of chiral primary amines.[1,2] Using an appropriate amine donor, the carbonyl group of a substrate is converted into an amine group, generating a primary amine mediated by the cofactor pyridoxal-5′-phosphate (PLP).[3–5]

One of the most challenging aspects utilizing transaminases is their catalytic performance in bulk substrate solution.[6] To increase the catalytic efficiency of transaminases for the synthesis of pharmaceuticals, extensive protein engineering is frequently necessary.[7,8]

A recent example for the use of biocatalytic transamination in the manufacture of APIs is the synthesis of the advanced intermediate **2** (Scheme 1) in one of the described commercial routes to sacubitril valsartan sodium hydrate, a medication used to treat heart failure.[8,9] The engineered ω-transaminase CDX-043 catalyzes the transamination of the substrate γ-keto acid **1**—present as the corresponding isopropyl ammonium salt—to the product γ-amino acid **2**. As transaminases may experience substrate and by-product inhibition,[10,11] a follow-up study for the transamination reaction catalyzed by CDX-043 was initiated to improve the understanding of kinetic and thermodynamic aspects of the process.

As the conversion in transamination reactions is frequently limited by the existence of a thermodynamic equilibrium between substrate and product, knowledge on the equilibrium position allows the identification of suitable process and engineering solutions, for example, the necessity of product removal[12] to maximize conversion and thus increase the isolated yield. Furthermore, precise investigation of the kinetics of the transamination reaction provides a deeper insight into the limits of productivity and the extent of substrate and/or product inhibition, enabling optimization of process conditions and the implementation of an appropriate reactor concept.

2. Results and Discussion

To confirm reversibility of the transamination reaction under the chosen reaction conditions, the thermodynamic equilibrium constant, K, was calculated from the final concentrations, c (mM), of substrate **1**, product **2**, amine donor isopropylamine (IPA), and by-product acetone that were reached after extended reaction times (Equation (1)).

$$K = \frac{[c_{\gamma\text{-amino acid}}] \cdot [c_{\text{acetone}}]}{[c_{\gamma\text{-keto acid}}] \cdot [c_{\text{IPA}}]} \quad (1)$$

[a] Z. Perçin, P. Bubenheim, A. Liese
Institute of Technical Biocatalysis, Hamburg University of Technology, Denickestraße 15 21073, Hamburg, Germany
E-mail: zeynep.percin@tuhh.de
liese@tuhh.de

[b] F. Kleinbeck, T. Ruch
Chemical & Analytical Development, Novartis Pharma AG, Basel 4056, Switzerland

Supporting information for this article is available on the WWW under https://doi.org/10.1002/cctc.202401405

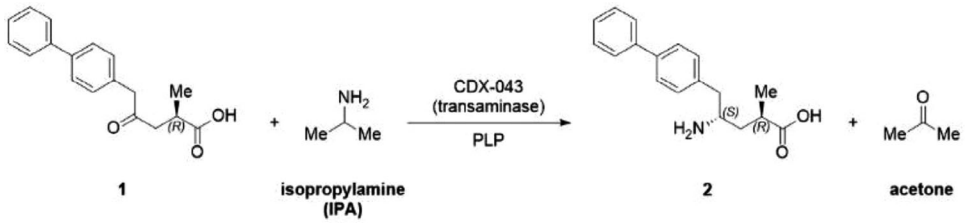

Scheme 1. Biocatalytic transformation of γ-keto acid **1** to γ-amino acid **2** by the transaminase CDX-043 using isopropylamine (IPA) as amine donor catalyzed using the cofactor pyridoxal 5′-phosphate (PLP). Acetone is produced as a by-product.

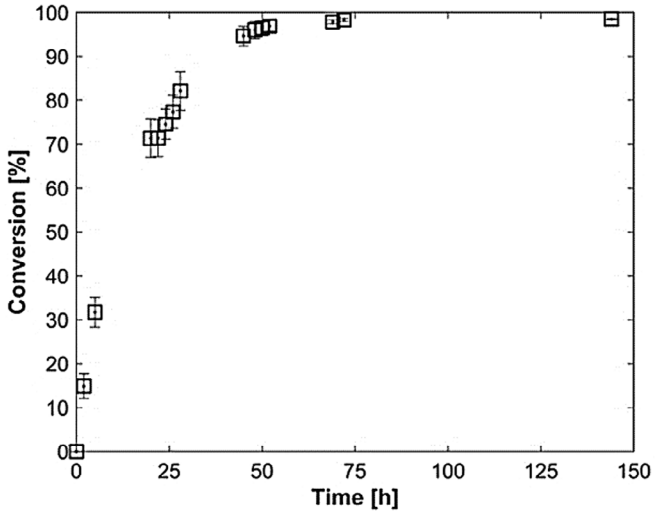

Figure 1. Experimental determination of the equilibrium position. Experimental conditions: 0.37 mg mL^{-1} of CDX-043, 58 °C, pH 8.5, 183 rpm (magnetic stirring), 241 ± 25 mM γ-keto acid **1**, 1510 mM IPA, reaction volume 0.75 mL (see the Supporting Information for details). All experiments were performed in duplicate. The data points after a reaction time of 45 h were obtained from a single experiment with duplicate sampling.

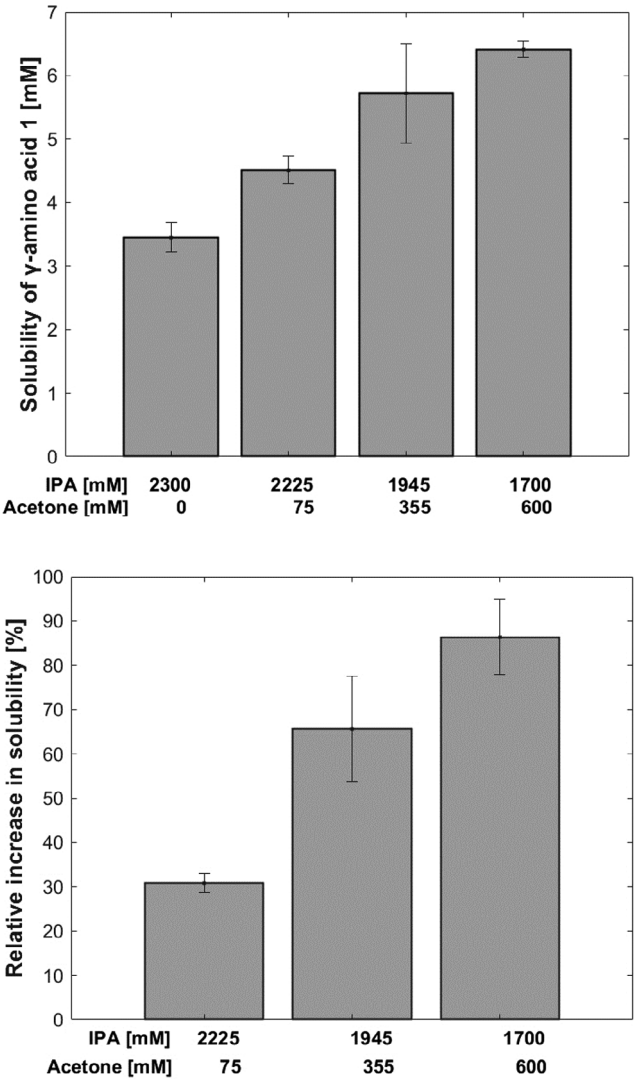

Figure 2. Solubility (top) and relative increase of solubility (bottom) of γ-amino acid **2** as a function of the concentration of by-product acetone. All experiments were performed in duplicate (see the Supporting Information for details).

To overcome the often unfavorable equilibrium in transamination reactions, favoring the ketone substrate over the amine product, the amine donor is typically applied in excess to achieve high conversion.[6,12–14] Due to the nature of the specific transformation investigated in this study, a smaller excess of only 6.3 equivalents of IPA was found to be sufficient to reach a conversion of 98.5 ± 0.1% (Figure 1) after 144 h, resulting in an equilibrium constant of 11.1 ± 0.

As illustrated in Scheme 1, the substrate γ-keto acid **1** and amine donor IPA react in a 1:1 stoichiometric ratio to give one equivalent each of the product γ-amino acid **2** and by-product acetone. The initial and final concentrations of γ-keto acid **1** were experimentally measured by HPLC in duplicate, whereas the concentrations of γ-amino acid **2**, IPA, and acetone were calculated based on the input quantity of IPA and the reaction stoichiometry. The margin of error was determined as the standard deviation of the duplicate measurements (Table 1).

Due to the lower solubility of product **2** compared to substrate **1** in the aqueous reaction mixture, the equilibrium of the reaction is inherently shifted towards the product side.[9] As the concentration of by-product acetone, a polar organic solvent fully miscible with water, increases with progressing conversion, the solubility of product **2** may potentially change over the course of the reaction. The effect of the concentration of by-product acetone on the solubility of γ-amino acid **2** utilizing excess amine donor was, therefore, experimentally investigated (Figure 2). In an initial experiment, the solubility was determined in the supernatant solution of suspended γ-amino acid **2** (nominal concentration of 8 mg mL^{-1}) in the bulk reaction medium in

Table 1. Equilibrium concentrations of reaction components.

	γ-Keto Acid 1	IPA	γ-Amino Acid 2	Acetone
$C_{initial}$ [mM]	241 ± 25	1510	0	
$C_{equilibrium}$ [mM]	3.4 ± 0.5	1290 ± 14	221 ± 14	221 ± 14
$C_{equilibrium}$ [mM], considering γ-amino acid **2** solubility limit	3.4 ± 0.5	1290 ± 14	2.3 ± 0.1	221 ± 14

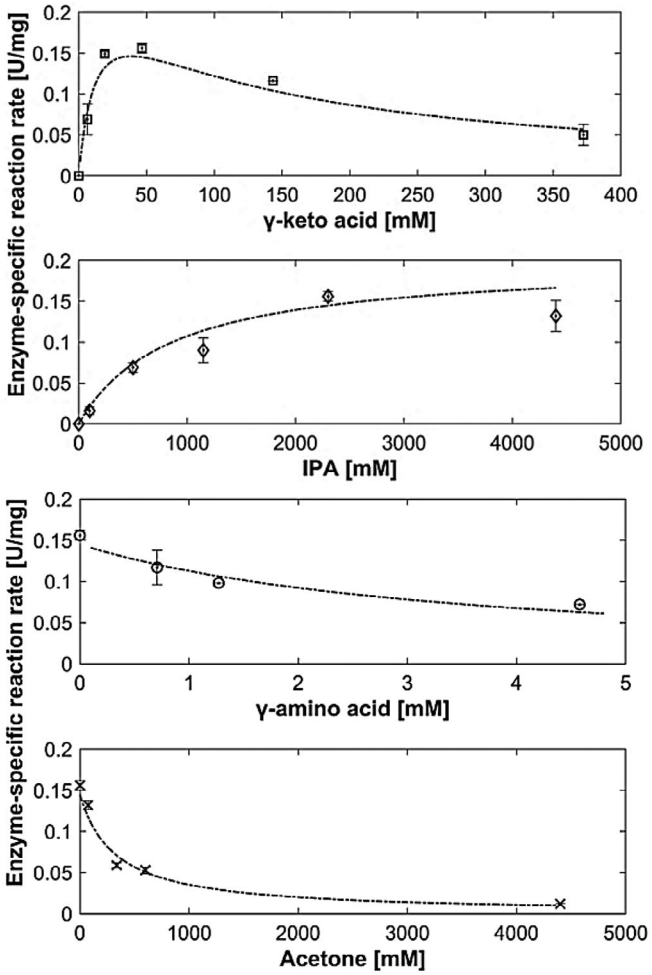

Figure 3. Kinetic models for initial reaction rate measurements of each reaction component. The dashed lines were fitted with Matlab R2023a to the experimental data using the kinetic parameters determined with Origin 2023b according to Equation (4). Experimental conditions: 0.37 mg mL^{-1} of CDX-043, 58 °C, pH 8.5, 183 rpm (magnetic stirring), reaction volume 0.75 mL (see the Supporting Information for details). All experiments were performed in duplicate, except for the last two data points of γ-amino acid 2 and the last data point of acetone, which were obtained in single experiments.

the absence of acetone at a concentration of 2300 mM of IPA, the IPA concentration at which the maximum reaction rate is achieved (Figure 3). This concentration was taken as the overall concentration of IPA and acetone for subsequent solubility determinations applying different ratios of IPA and acetone, gradually increasing the acetone to simulate progressing conversion and concomitant formation of acetone as a by-product of the reaction. Solubility of product **2** was found to increase as a function of the acetone concentration, highlighting that the by-product

Table 2. Kinetic parameters obtained from the modified design equations of the evaluated ping-pong two-substrate and Michaelis–Menten double substrate kinetic models and the catalytic efficiency of the engineered transaminase CDX-043.

	Ping-Pong	Michaelis–Menten
$K_{m,\gamma\text{-keto acid}}$ [mM]	15.9 ± 8.7	13.3 ± 6.9
$K_{m,IPA}$ [mM]	800 ± 725	851 ± 338
V_{max} [U mg^{-1}]	0.3 ± 0.1	0.3 ± 0.1
$K_{i,\gamma\text{-keto acid}}$ [mM]	38.3 ± 37.5	112 ± 56
$K_{i,acetone}$ [mM]	52.9 ± 24.5	54 ± 23
$K_{i,\gamma\text{-amino acid}}$ [mM]	1.3 ± 0.6	0.6 ± 0.3
R^2	0.9251	0.9347
$\frac{K_{m,\gamma\text{-keto acid}}}{K_{i,\gamma\text{-amino acid}}}$	11.6 ± 1.4	21.8 ± 2.0
$\frac{K_{m,\gamma\text{-keto acid}}}{K_{i,acetone}}$	0.3 ± 0.0	0.2 ± 0.0

acetone acts as a cosolvent and thus resulting in increased solubility of the γ-amino acid **2** over the course of the reaction (Figure 2).

To quantify the apparent equilibrium constant, it was necessary to consider the concentration of the product γ-amino acid **2** solubilized in the reaction medium. The acetone concentration was fitted to Equation (2) ($R^2 = 0.976$), thereby establishing a correlation between the acetone concentration from Figure 3 and the product solubility. The concentration of γ-amino acid **2** was calculated as 2.3 ± 0.1 mM (Table 2). Accordingly, an equilibrium constant of 0.12 ± 0.0 was calculated on the basis of the solubility limitations of γ-amino acid **2**.

$$c_{\gamma-\text{amino acid}} = -0.000007 \cdot (c_{\text{acetone}})^2 + 0.008 \cdot c_{\text{acetone}} + 3.629 \quad (2)$$

This finding emphasizes the effect of phase separation, which is relevant for the product γ-amino acid **2**. As a result, the equilibrium constant (0.12 ± 0.00) is lower than the theoretical value (11.1 ± 0.0), indicating that the required excess of the amine donor IPA was significantly decreased in accordance with the literature.[12]

To identify potential inhibition of the transaminase enzyme, the affinity of each reaction component—substrate γ-keto acid **1**, product γ-amino acid **2**, amine donor IPA, and by-product acetone—for CDX-043 was investigated by initial rate measurements (see the Supporting Information for details). The results of the kinetic measurements are summarized in Figure 3.

The Michaelis–Menten kinetic model provides a nonmechanistic description of the interaction between an enzyme and its substrate, which results in the formation of an enzyme–substrate

complex. The complex then facilitates the release of the product, which in turn initiates the regeneration of the original form of the enzyme. The ping-pong two-substrate (ping-pong bi–bi) kinetic model applied for the transamination reaction is a mechanistic model that describes the order of adsorption and desorption of substrates and products from the active site. Here, it proposes that the PLP cofactor forms a complex with the enzyme ω-transaminase, which facilitates the production of acetone from isopropyl alcohol (IPA). Subsequently, the transfer of the amino group from the amine donor (IPA) to the amine acceptor γ-keto acid **1** occurs, resulting in the formation of the product γ-amino acid **2**. The complex then facilitates the release of γ-amino acid **2**, which in turn initiates the regeneration of the original form of the enzyme–PLP complex.

Values of $K_{m,\gamma\text{-keto acid}}/K_i$ lower than 1 indicate satisfactory efficiency, as the affinity of the substrate γ-keto acid **1** is greater than the inhibition of the enzyme by the respective reaction product, whereas values higher than 1 indicate product inhibition dominating over substrate affinity. For acetone, reaction efficiencies below 1 are found for both kinetic models. However, the opposite is the case for γ-amino acid **2**, with values above 1 indicating that the rate of the forward reaction, that is, the conversion of γ-keto acid **1** to γ-amino acid **2** slows down as the reaction progresses, and the substrate concentration drops below the Michaelis–Menten constant ($c_S < K_m$).[15]

The kinetic parameters were determined using Origin 2023b by fitting the experimental data from the initial rate measurements to Equations (3) and (4) for the two kinetic models.[16,17] The kinetic parameters obtained for the two kinetic models are listed in Table 2. The reaction efficiency, defined as $K_{m,\gamma\text{-keto acid}}/K_i$, the ratio of the Michaelis–Menten constant of the γ-keto acid **1** to the inhibition constant of the reaction products,[18,19] was calculated for the product γ-amino acid **2** and the by-product acetone (Table 2).

In order for biocatalytic reactions with two substrates to run at a constant rate, both substrates must be present at concentrations exceeding the Michaelis–Menten constants of each substrate to ensure saturation of the enzyme (zero order kinetics).[20,21] If the enzyme is not saturated with its substrates during the course of the reaction, the rate of reaction will be negatively affected.[22,23] The determined kinetic parameters, specifically $K_{m,\gamma\text{-keto acid}}$ and $K_{m,IPA}$ for both the ping-pong two-substrate and Michaelis–Menten double substrate kinetic models, indicate that saturation with both substrates is observed as the substrate concentrations exceed the minimum substrate concentration at which saturation of the transaminase with both substrates occurs. Therefore, no further investigations were performed to optimize the concentration of γ-keto acid **1**.

The effect of severe inhibition can be overcome by the selection of an appropriate reactor design. The studies on enzyme inhibition demonstrated a more pronounced inhibitory effect for the product γ-amino acid **2** than for the by-product acetone or the substrate γ-keto acid **1**, as seen by comparison of the inhibition constants (Table 2). The same reduction of the enzyme-specific reaction rate is thus observed at a significantly lower concentration of γ-amino acid **2** than for the by-product acetone or the substrate γ-keto acid **1** (Figure 3). Therefore, a low product concentration is beneficial and could be achieved by the use of a plug flow reactor (PFR). In a PFR, the product concentration is lowest at the inlet of the reactor and increasing over the length of it in contrast to a CSTR, operating under outflow conditions at highest possible product concentration all the time. In consequence, in the PFR the transaminase enzyme is exposed to highly concentrated product only at the outlet.[24,25] On the contrary, if substrate surplus inhibition was dominant, a continuous stirred tank reactor (CSTR) would be the option of choice because the substrate is diluted in a CSTR. Due to the physical properties of the viscous reaction mixture, a PFR was not further investigated for process development in this work.

For comparison of the two reactor options, CSTR and PFR, the performance of the reaction in both setups was simulated. Comparison was based on the dimensionless operation time required to obtain a target conversion at the same reactor volume and enzyme concentration, assuming that enzyme activity is constant and independent of the reaction time. The dimensionless operation time was calculated according to Equation (5),[26] where m_{cat} is the enzyme load (mg mL^{-1}), ν is the transaminase-specific reaction rate (U mg^{-1}), $\dot{V}$ represents the flow rate of the reaction mixture (mL min^{-1}), and V_R is the reactor volume (mL).

$$\text{Dimensionless operation time}\,[-] = \frac{m_{cat} \cdot \nu \cdot V_R}{\dot{V} \cdot K_{m,\gamma-\text{keto acid}}} \tag{5}$$

As determination of the dimensionless operating time requires calculation of the reaction rate, it is critical to identify the kinetic model matching closest with the experimental data. For the purpose of comparison, both kinetic models were simulated using the design equation of a batch reactor according to Equation (6). The simulation and experimental results are illustrated in Figure 4, where v is the transaminase-specific reaction rate (U mg^{-1}) and c is the transaminase concentration (mg mL^{-1}).

$$\frac{dc_{\gamma-\text{keto acid}}}{dt} = -\nu \cdot c_E \tag{6}$$

For the Michaelis–Menten double substrate kinetic model to match the experimental data, an enzyme concentration c_E of 13 mg mL^{-1} would be required, which is 35 times higher

$$v = \frac{v_{max} \cdot [c_{\gamma-\text{keto acid}}] \cdot [c_{IPA}]}{K_{m,\gamma-\text{keto acid}} \cdot [c_{IPA}] \cdot [1+C_{acetone}/K_{i,acetone}] + K_{m,IPA} \cdot [c_{\gamma-\text{keto acid}}] \cdot [1+c_{\gamma-\text{keto acid}}/K_{i,\gamma-\text{keto acid}}] \cdot [1 + c_{\gamma-\text{amino acid}}/K_{i,\gamma-\text{amino acid}}] + [c_{IPA}] \cdot [c_{\gamma-\text{keto acid}}]} \tag{3}$$

$$v = \frac{v_{max} \cdot [c_{\gamma-\text{keto acid}}] \cdot [c_{IPA}]}{\left(K_{m,\gamma-\text{keto acid}} \cdot [1 + c_{acetone}/K_{i,acetone}] \cdot [1+c_{\gamma-\text{amino acid}}/K_{i,\gamma-\text{amino acid}}] + [c_{\gamma-\text{keto acid}}] + [c_{\gamma-\text{keto acid}}]^2/K_{i,\gamma-\text{keto acid}}\right) + (K_{m,IPA} + [c_{IPA}])} \tag{4}$$

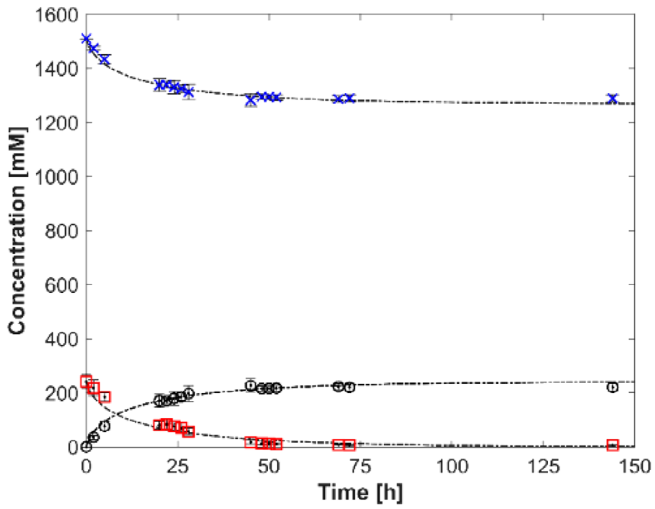

Figure 4. Simulation and experimental results for the batch operation mode at the same initial concentration of substrate **1**. All simulations, represented by dashed lines, were performed according to Equation (4) using Matlab R2023a (see Figure 1 for experimental conditions). Data points are based on experimental results and are shown as symbols (blue crosses = IPA calculated; red squares = γ-keto acid **1** measured; and black circles = γ-amino acid **2** calculated).

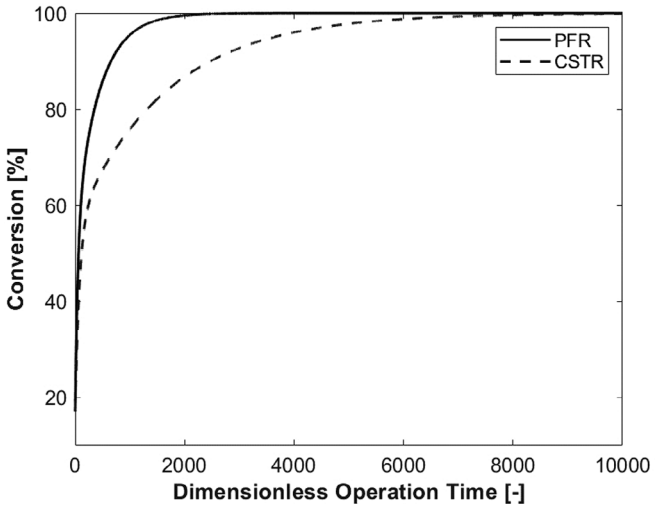

Figure 5. Comparison of dimensionless operation time for PFR (solid) and CSTR (dashed) at given conversion values calculated using the Michaelis–Menten constant $K_{m,\gamma\text{-keto acid}}$ of γ-keto acid **1**. Initial conditions for simulation: 241 mM γ-keto acid 1, 1510 mM IPA; simulated operating conditions: 13 mg mL^{-1} of CDX-043, reaction volume 1000 mL for both PFR and CSTR.

than the actual concentration based on the charging quantity of the enzyme in the experiments. The coefficient of determination (0.93) was calculated considering measured and predicted γ-keto acid **1** concentrations. In comparison, a 135-fold higher enzyme concentration c_E of 50 mg mL^{-1} would be needed to obtain a comparable data fit with a coefficient of determination of 0.93.

Both the Michaelis–Menten double-substrate and the ping-pong two-substrate kinetic models were modified by the addition of inhibition constants, designated $1 + C_{inhibitor}/K_{inhibitor}$ in Equations (2) and (3), to each original model equation. To ensure an adequate fit of the simulations to the experimental data, a higher enzyme concentration than experimentally applied during the kinetic studies needs to be reflected for each kinetic model and obtain an accurate quantitative description of the system. The experiment was conducted over a period of 100 h, during which the enzyme deactivation in the reaction rate modelling was not considered. This could result in the use of an increased enzyme concentration when the modeled reaction rate is fitted to the experimental data. When comparing the two kinetic models, the Michaelis–Menten two-substrate kinetic model requires a lower enzyme concentration than the ping-pong two-substrate kinetic model to fit the experimental data at the same coefficient of determination, indicating that the Michaelis–Menten two-substrate kinetic model fits better for the transaminase reaction.

The concentrations of the γ-keto acid **1** and the γ-amino acid **2** were appropriately selected to estimate the kinetic parameters as high substrate concentration and low product concentration are required to investigate uncompetitive inhibition and competitive inhibition, respectively.[21] The reaction rate equation (Equation (6)) for the Michaelis–Menten double substrate kinetic model was implemented in the design equations for PFR (Equation (7)) and for CSTR (Equation (8)) using the kinetic parameters from Table 2, where L is the length (m) and A is the cross-sectional area (m^2) of the PFR.

$$\text{PFR} \quad \frac{dc_{\gamma-\text{keto acid}}}{dL} = \frac{-\nu \cdot c_E}{\dot{V}} \cdot A \tag{7}$$

$$\text{CSTR} \quad \frac{dc_{\gamma-\text{keto acid}}}{dt} = \frac{\dot{V}}{V_R} \cdot \left(c_{\text{keto acid}(t=0)} - (t)\right) - \nu \cdot C_E \tag{8}$$

The conversions were then compared under the same process conditions (Figure 5), showing that for the PFR, maximum conversion is achieved in a shorter time and at a lower total enzyme load, as the PFR provides a higher volumetric conversion.

3. Conclusion

Fundamental thermodynamic and kinetic aspects of the transamination reaction of γ-keto acid **1** and the γ-amino acid **2** using the transaminase CDX-043 were investigated. The existence of an equilibrium between γ-keto acid **1** to the γ-amino acid **2** was experimentally proven. A kinetic model considering substrate and product inhibition was developed by comparison of the Ping-pong two-substrate and the Michaelis–Menten double substrate kinetic models, showing better agreement of the Michaelis–Menten model with experimental results. Competitive inhibition at lower concentration of γ-amino acid **2** was identified. Furthermore, the biocatalytic efficiency of CDX-043 was determined. Finally, the kinetic model developed was used to select the appropriate reactor concept, considering the benefits of continuous flow reactors in light of product inhibition. The performance of plug flow reactor (PFR) and continuous stirred tank reactor (CSTR) were compared by

simulation, demonstrating PFR to be the optimum mode of operation.

The Michaelis–Menten kinetic model in this study can be applied to other transamination reactions to estimate and optimize reaction performance. The study demonstrates the value of detailed investigations of reaction thermodynamics and kinetics to improve biocatalytic transformations for industrial application.

Supporting Information

The Supporting Information for this article provides details on experimental protocols, HPLC analyses, and sample preparation.

Acknowledgments

The authors acknowledge Uta Naefken for her help in the laboratory.

Conflict of Interests

The authors declare no conflict of interest.

Data Availability Statement

The data that support the findings of this study are available from the corresponding author upon reasonable request.

Keywords: Biotransformation · Kinetic models · Optimization · Reactor selection · ω-Transaminase

[1] S. A. Kelly, S. Pohle, S. Wharry, S. Mix, C. C. R. Allen, T. S. Moody, B. F. Gilmore, *Chem. Rev.* **2018**, *118*, 349–367.
[2] S. A. Kelly, S. Mix, T. S. Moody, B. F. Gilmore, *Appl. Microbiol. Biotechnol.* **2020**, *104*, 4781–4794.
[3] S. Wu, R. Snajdrova, J. C. Moore, K. Baldenius, U. T. Bornscheuer, *Angew. Chem. Int. Ed.* **2021**, *60*, 88–119.
[4] R. Buller, S. Lutz, R. J. Kazlauskas, R. Snajdrova, J. C. Moore, U. T. Bornscheuer, *Science* **2023**, *382*, eadh8615.
[5] G. Matcham, M. Bhatia, W. Lang, C. Lewis, R. Nelson, A. Wang, W. Wu, *Chimia* **1999**, *53*, 584–589.
[6] L. Yang, K. Zhang, M. Xu, Y. Xie, X. Meng, H. Wang, D. Wei, *Angew. Chem., Int. Ed.* **2022**, *61*, e202212555.
[7] M. S. Weiß, I. V. Pavlidis, P. Spurr, S. P. Hanlon, B. Wirz, H. Iding, U. T. Bornscheuer, *Org. Biomol. Chem.* **2016**, *14*, 10249–10254.
[8] S. J. Novick, N. Dellas, R. Garcia, C. Ching, A. Bautista, D. Homan, O. Alvizo, D. Entwistle, F. Kleinbeck, T. Schlama, T. Ruch, *ACS Catal.* **2021**, *11*, 3762–3770.
[9] X. Gu, J. Zhao, L. Chen, Y. Li, B. Yu, X. Tian, Z. Min, S. Xu, H. Gu, J. Sun, X. Lu, M. Chang, X. Wang, L. Zhao, S. Ye, H. Yang, Y. Tian, F. Gao, Y. Gai, G. Jia, J. Wu, Y. Wang, J. Zhang, X. Zhang, W. Liu, X. Gu, X. Luo, H. Dong, H. Wang, B. Schenkel, F. Venturoni, P. Filipponi, B. Guelat, T. Allmendinger, B. Wietfeld, P. Hoehn, N. Kovacic, L. Hermann, T. Schlama, T. Ruch, N. Derrien, P. Piechon, F. Kleinbeck, *J. Org. Chem.* **2020**, *85*, 6844–6853.
[10] J.-S. Shin, B.-G. Kim, *Biotechnol. Bioeng.* **2002**, *77*, 832–837.
[11] C. A. Gal, L.-E. Barabás, A. Varga, P. Csuka, L. C. Bencze, M. L. Toşa, L. Poppe, C. Paizs, *Mol. Catal.* **2022**, *531*, 112660.
[12] P. Tufvesson, J. Lima-Ramos, J. S. Jensen, N. Al-Haque, W. Neto, J. M. Woodley, *Biotechnol. Bioeng.* **2011**, *108*, 1479–1493.
[13] C. K. Savile, J. M. Janey, E. C. Mundorff, J. C. Moore, S. Tam, W. R. Jarvis, J. C. Colbeck, A. Krebber, F. J. Fleit, J. Brands, P. N. Devine, G. W. Huisman, G. J. Hughes, *Science* **2010**, *329*, 305–309.
[14] M. Truppo, J. M. Janey, B. Grau, K. Morley, S. Pollack, G. Hughes, I. Davies, *Catal. Sci. Technol.* **2012**, *2*, 1556–1559.
[15] M. D. Gomes, J. M. Woodley, *Molecules* **2019**, *24*, 3573.
[16] V. Leskovac, *Comprehensive Enzyme Kinetics*, Kluwer Academic/Plenum Publishers, New York, **2003**, p. 200.
[17] D. Vasic-Racki, A. Liese, U. Kragl, *Chem. Biochem. Eng. Q.* **2003**, *17*, 3–14.
[18] L. G. Lee, G. M. Whitesides, *J. Am. Chem. Soc.* **1985**, *107*, 6999–7008.
[19] A. Liese, M. Karutz, J. Kamphuis, C. Wandrey, U. Kragl, *Biotechnol. Bioeng.* **1996**, *51*, 544–550.
[20] C. Park, *J. Chem. Educ.* **2022**, *99*, 2556–2562.
[21] A. Cornish-Bowden, *Perspect. Sci.* **2014**, *1–6*, 121–125.
[22] A. Toftgaard Pedersen, W. R. Birmingham, G. Rehn, S. J. Charnock, N. J. Turner, J. M. Woodley, *Org. Process Res. Dev.* **2015**, *19*, 1580–1589.
[23] P. K. Robinson, *Essays Biochem.* **2015**, *59*, 1–41.
[24] K. Mårtensson, *Appl. Biochem. Biotechnol.* **1982**, *7*, 11–18.
[25] R. M. Lindeque, J. M. Woodley, *CatalystsCatalysts* **2019**, *9*, 262.
[26] A. Illanes, L. Wilson, C. Vera, *Problem Solving in Enzyme Biocatalysis*, John Wiley & Sons, Ltd., Chichester, United Kingdom, **2014**, p. 144.

Manuscript received: August 19, 2024
Revised manuscript received: October 27, 2024
Accepted manuscript online: November 19, 2024
Version of record online: November 30, 2024